The Plant Cell, Vol. 25: 3743–3759, October 2013, www.plantcell.org

RESEARCH ARTICLES

Genome-Wide Binding Analysis of the Transcription Activator IDEAL PLANT ARCHITECTURE1 Reveals a Complex Network Regulating Rice Plant Architecture[W]

Zefu Lu,[a,1] Hong Yu,[a,1] Guosheng Xiong,[a,1] Jing Wang,[a,2] Yongqing Jiao,[a,3] Guifu Liu,[a] Yanhui Jing,[a] Xiangbing Meng,[a] Xingming Hu,[b] Qian Qian,[b] Xiangdong Fu,[c] Yonghong Wang,[a] and Jiayang Li[a,4]

[a] State Key Laboratory of Plant Genomics and National Center for Plant Gene Research (Beijing), Institute of Genetics and Developmental Biology, Chinese Academy of Sciences, Beijing 100101, China

[b] State Key Laboratory of Rice Biology, China National Rice Research Institute, Hangzhou 310006, China

[c] State Key Laboratory of Plant Cell and Chromosome Engineering and National Center for Plant Gene Research (Beijing), Institute of Genetics and Developmental Biology, Chinese Academy of Sciences, Beijing 100101, China

ORCID IDs: 0000-0001-9322-8351 (Z.L.); 0000-0002-1748-8693 (H.Y.); 0000-0001-9857-7542 (G.X.); 0000-0002-0487-6574 (J.L.).

IDEAL PLANT ARCHITECTURE1* (*IPA1*) is critical in regulating rice (*Oryza sativa*) plant architecture and substantially enhances grain yield. To elucidate its molecular basis, we first confirmed IPA1 as a functional transcription activator and then identified 1067 and 2185 genes associated with IPA1 binding sites in shoot apices and young panicles, respectively, through chromatin immunoprecipitation sequencing assays. The SQUAMOSA PROMOTER BINDING PROTEIN-box direct binding core motif GTAC was highly enriched in IPA1 binding peaks; interestingly, a previously uncharacterized indirect binding motif TGGGCC/T was found to be significantly enriched through the interaction of IPA1 with proliferating cell nuclear antigen PROMOTER BINDING FACTOR1 or PROMOTER BINDING FACTOR2. Genome-wide expression profiling by RNA sequencing revealed IPA1 roles in diverse pathways. Moreover, our results demonstrated that IPA1 could directly bind to the promoter of rice *TEOSINTE BRANCHED1*, a negative regulator of tiller bud outgrowth, to suppress rice tillering, and directly and positively regulate *DENSE AND ERECT PANICLE1*, an important gene regulating panicle architecture, to influence plant height and panicle length. The elucidation of target genes of *IPA1* genome-wide will contribute to understanding the molecular mechanisms underlying plant architecture and to facilitating the breeding of elite varieties with ideal plant architecture.

INTRODUCTION

Rice (*Oryza sativa*) plant architecture, including plant height, tiller number, tiller angle, and panicle morphology, is one of the major factors that determine grain productivity (Wang and Li, 2008). Based on recent studies on rice mutants, many important genes involved in regulating plant architecture have been characterized. Genes such as *ELONGATED UPPERMOST INTERNODE1* (*EUI1*), *SEMI DWARF1*, *SLENDER RICE1* (*SLR1*), *GA-INSENSITIVE DWARF1* (*GID1*), and *GID2* are found to be important components of the gibberellic acid biosynthetic and signal transduction pathways regulating plant height (Ikeda et al., 2001; Sasaki et al., 2002, 2003; Ueguchi-Tanaka et al., 2005; Zhu et al., 2006). The *DWARF* genes, including *D3*, *D10*, *D14*, *D17*, and *D27*, have been found to play critical roles in the strigolactone biosynthesis or signal transduction pathways influencing rice tiller number (Ishikawa et al., 2005; Zou et al., 2005; Arite et al., 2007, 2009; Lin et al., 2009). *TEOSINTE BRANCHED1* (*TB1*), a member of the TEOSINTE BRANCHED1, CYCLOIDEA AND PCF TRANSCRIPTION FACTOR (TCP) gene family, functions as a negative regulator of lateral branching in rice that acts downstream of *DWARF* to repress the outgrowth of axillary buds (Takeda et al., 2003; Minakuchi et al., 2010). For the regulation of panicle morphology, LONELY GUY (LOG) and GRAIN NUMBER1a/CYTOKININ OXIDASE2, two components of the cytokinin metabolic pathway, play important roles in the development of panicle branches (Ashikari et al., 2005; Kurakawa et al., 2007). *DENSE AND ERECT PANICLE1* (*DEP1*) encodes a phosphatidylethanolamine binding protein–like domain protein. Rice varieties carrying the *dep1* mutation, a dominant allele at the *DEP1* locus, exhibit reduced length of inflorescence internodes, increased number of grains per panicle, and enhanced grain yield (Huang et al., 2009). Recently, more genes involved in the regulation of rice architecture have been characterized, such as *DEP3*, *RICE LEAFY HOMOLOG*, *MADS-BOX TRANSCRIPTION FACTOR57* (*MADS57*), and *SQUAMOSA PROMOTER BINDING-LIKE PROTEIN16* (*SPL16*) (Rao et al., 2008; Qiao et al., 2011; Wang et al., 2012; Guo et al., 2013). However, the molecular mechanisms underlying plant architecture remain unclear.

To meet the increasing demand for food, the concept of ideal plant architecture or new plant type has been proposed since

[1] These authors contributed equally to this work.

[2] Current address: Rice Research Institute, Sichuan Agricultural University, Sichuan 611130, China.

[3] Current address: Division of Plant Sciences and National Center for Soybean Biotechnology, University of Missouri, Columbia, MO 65211.

[4] Address correspondence to jyli@genetics.ac.cn.

The author responsible for distribution of materials integral to the findings presented in this article in accordance with the policy described in the Instructions for Authors (www.plantcell.org) is: Jiayang Li (jyli@genetics.ac.cn).

[W] Online version contains Web-only data.

www.plantcell.org/cgi/doi/10.1105/tpc.113.113639

the sixties of the last century (Donald, 1968; Khush, 1995). Features of ideal plant architecture include low tiller number, few unproductive tillers, more grains per panicle, stronger culms, and robust roots (Khush, 1995; Virk et al., 2004). *IDEAL PLANT ARCHITECTURE1* (*IPA1*), a pleiotropic gene isolated through a map-based cloning approach, has been shown to be one of the key regulators that determine plant architecture (Jiao et al., 2010). *IPA1* encodes the protein Os SPL14, and in the *ipa1* mutant, one nucleotide substitution located in the recognition site for microRNA156 (miRNA156) perturbs *IPA1* mRNA degradation, which results in accumulation of IPA1 and leads to the formation of ideal plant architecture with decreased tiller number and increased plant height and panicle branches (Jiao et al., 2010). *WEALTHY FARMER'S PANICLE*, another overexpression allele of Os *SPL14*, resulted from an epigenetic change in the Os *SPL14* promoter and shows a similar phenotype (Miura et al., 2010). Therefore, it has been suggested that Os *SPL14* alleles have great potential for breeding (Jiao et al., 2010; Miura et al., 2010). However, how *IPA1* affects plant architecture and whether any relationship exists between *IPA1* and other plant architecture regulation genes remain largely unknown.

SPL proteins are plant specific and share a highly conserved zinc ion–containing DNA binding domain named the SQUAMOSA PROMOTER BINDING PROTEIN (SBP)-box (Yamasaki et al., 2004). A 4-bp sequence (GTAC) is the core binding motif of the SBP-box and is also the copper ion response element (Birkenbihl et al., 2005). In *Arabidopsis thaliana*, most of the *SPL* genes are targets of miRNA156 (Fornara and Coupland, 2009; Wang et al., 2009; Yamaguchi et al., 2009). The *SPL* genes are reported to be important components in the regulation of various developmental processes. *SPL3*, the homolog of snapdragon *SBP1*, can directly bind to the promoters of *LEAFY* (*LFY*), *FRUITFULL*, and *APETALA1* and promote the expression of *FLOWERING LOCUS T* (*FT*) to induce phase transition (Wu and Poethig, 2006; Gandikota et al., 2007; Yamaguchi et al., 2009). *SPL9*, the *Arabidopsis* ortholog of *IPA1*, targets the promoter of the *miRNA172* precursor and regulates the expression of *AGAMOUS LIKE42* (*AGL42*), *SUPPRESSOR OF OVEREXPRESSION OF CONSTANS1* (*SOC1*), and *FT* (Fornara and Coupland, 2009; Wang et al., 2009; Wu et al., 2009). Besides their roles in phase transition, *SPL* genes also participate in regulation of microspore development, trichome development, and anthocyanin biosynthesis (Unte et al., 2003; Yu, N. et al., 2010; Gou et al., 2011). However, in grain crops, despite their importance to agriculture, little is known about the underlying molecular mechanism of *SPL* genes.

In recent years, chromatin immunoprecipitation (ChIP)-on-chip and ChIP followed by sequencing (ChIP-seq) have emerged as powerful tools to profile genome-wide direct target genes for pivotal plant transcription factors (Johnson et al., 2008; Valouev et al., 2008; Hu et al., 2010). In *Arabidopsis*, genome-wide direct target gene analyses for key transcription factors, including *LFY*, *LONG HYPOCOTYL5*, *FAR-RED ELONGATED HYPOCOTYLS3*, *PHYTOCHROME INTERACTING FACTOR 3-LIKE5*, *AGL15*, *WUSHEL*, *BRASSINAZOLE RESISTANT1*, and *PHYTOCHROME INTERACTING FACTOR3*, have made large contributions to our knowledge about these key genes (Lee et al., 2007; Oh et al., 2007; Zheng et al., 2009; Busch et al., 2010; Sun et al., 2010; Winter et al., 2011; Zhang et al., 2013). In maize (*Zea mays*), the identification of KNOTTED1 target genes demonstrated that a key regulator can play a pivotal role in orchestrating hierarchical regulatory networks in monocots (Bolduc et al., 2012). Similarly, identification of genome-wide target genes for *IPA1* is particularly important for understanding the formation of ideal plant architecture and illustrating the functions of *SPL* genes in monocotyledonous plants.

Here, we report the identification of 1067 and 2185 genes that associate with IPA1 binding sites in shoot apices (SAs) and young panicles (YPs), respectively. IPA1 could directly bind to the SBP-box target motif GTAC and significantly enrich the TCP targeting motif TGGGCC/T through its interaction with proliferating cell nuclear antigen PROMOTER BINDING FACTOR1 (PCF1) and PCF2. Genome-wide expression profiling analysis and further characterization of the regulation by IPA1 of Os *TB1* and *DEP1* reveal key roles for IPA1 in the regulation of plant architecture and its involvement in other developmental processes. The unraveling of the genetic network orchestrated by *IPA1* contributes to elucidating the molecular mechanisms underlying plant architecture and facilitating the breeding of elite varieties with ideal plant architecture.

RESULTS

IPA1 Is a Functional Transcription Factor

IPA1 encodes a predicted member of the SPL family, which may function as a type of plant-specific transcription factors. To confirm whether IPA1 is a transcription factor, we performed a transcriptional activity assay in rice protoplasts and found that IPA1 had strong transactivation activity (Figure 1A), indicating that IPA1 functions as an activator in regulating gene expression. To further find out which part of IPA1 is responsible for the transcriptional activity, we performed a transcriptional activity assay in yeast (*Saccharomyces cerevisiae*) cells and found that the activation domain was located at the C-terminal region (Figure 1B). The iconic feature of SPL proteins is the conserved SBP-box. In *Arabidopsis*, the SBP-box contains a DNA binding domain, directly targeting a core sequence, GTAC (Birkenbihl et al., 2005). Gel electrophoresis mobility shift assays (EMSAs) were performed to test the DNA binding activity of IPA1. A core sequence containing GTAC was used as the target probe with a mutated core sequence containing ATAC as a negative control. As shown in Figure 1C, glutathione *S*-transferase (GST)-IPA1 could significantly reduce the electrophoretic mobility of the probe containing the GTAC motif and the addition of IPA1 antibodies could intensify the reduction, while the electrophoretic mobility of the mutated control probe was unaffected. These results demonstrated that IPA1 is a functional transcription factor with both DNA binding and transactivation activities.

IPA1 Binding Profiles at Two Developmental Stages

To further understand how *IPA1* regulates plant architecture, we systematically identified IPA1 target genes by investigating the global binding profiles of IPA1 in vivo. The ChIP-seq assay was performed using *ProIPA1:7mIPA1-GFP* (for green fluorescent protein) transgenic lines, which contain seven site substitutions

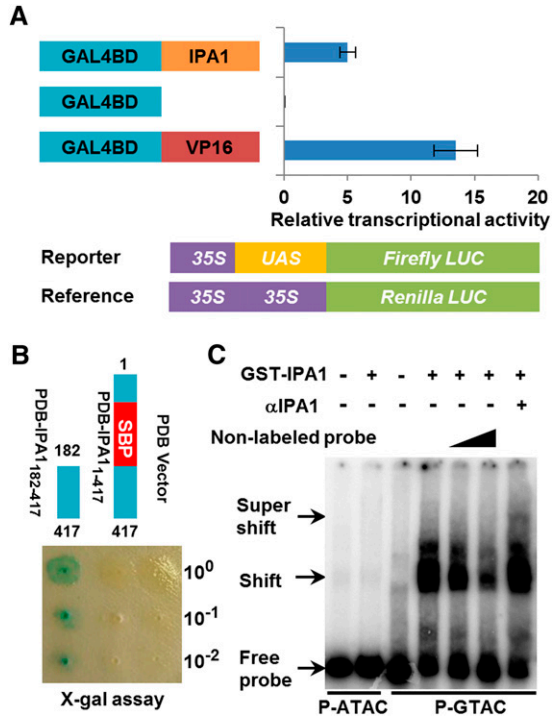

Figure 1. IPA1 Is a Transcriptional Activator.

(A) IPA1 shows strong transactivation activity in a transcriptional activity assay using rice protoplasts. IPA1 was fused to the GAL4 binding domain. Activities of firefly luciferase driven by the GAL4 binding element *UPSTREAM ACTIVATION SEQUENCE* (*UAS*) were measured. *Renilla* LUC was used as reference and VP16 as a positive control. Error bar indicates SE.

(B) Yeast cells expressing the C terminus of IPA1 significantly promoted the expression of β-galactosidase.

(C) IPA1 can directly bind to the core sequence in a GTAC-dependent manner. P-GTAC, a 59-bp probe containing the GTAC motif; P-ATAC, the negative control of P-GTAC. The 20- and 50-fold excess nonlabeled were used for competition.

that disturb the target sites of miRNA156 without changing the amino acid sequence of IPA1 and have few tillers and dense panicle phenotypes similar to the *ipa1* mutant (Jiao et al., 2010). Based on the *ipa1* phenotype, two representative tissues, SA and YP, were used to identify IPA1 target genes in ChIP-seq assays with two biological replicates (see Supplemental Figure 1 online). The qualities of all four ChIP-seq data sets were confirmed by cross-correlation metrics (see Supplemental Figure 2 online). Model-based analysis of ChIP-seq was then used to identify in vivo IPA1 binding sites, and genes that had IPA1 binding sites within the 500-bp promoter region and first intron were considered to be associated with IPA1 binding sites.

In both SA and YP, the two replicates shared a large number of target genes that covered more than 60% of the smaller set (Figure 2A), indicating high quality that was further tested for 14 randomly selected loci by ChIP–quantitative PCR (qPCR) (see Supplemental Figure 3 online). The overlapping peaks of two replicates were higher than nonoverlapping peaks in both SAs and YPs (see Supplemental Figure 4 online), indicating that using the overlapping peaks would keep the most robust IPA1 binding sites and further increase the accuracy of ChIP-seq results. Therefore, the common genes in both replicates were used, and a total of 1067 and 2185 genes associated with IPA1 binding sites in SAs and YPs, respectively, were found with 581 overlapping genes that accounted for 54.5% in SAs and 26.5% in YPs (Figure 2B; see Supplemental Data Sets 1A and 1B online). The number of unique genes in YPs was 1604, which was much larger than the 486 in SAs, indicating that more binding events take place in the panicle.

Further genome distribution analysis revealed that the IPA1 binding sites were highly enriched in the promoter region 3 kb

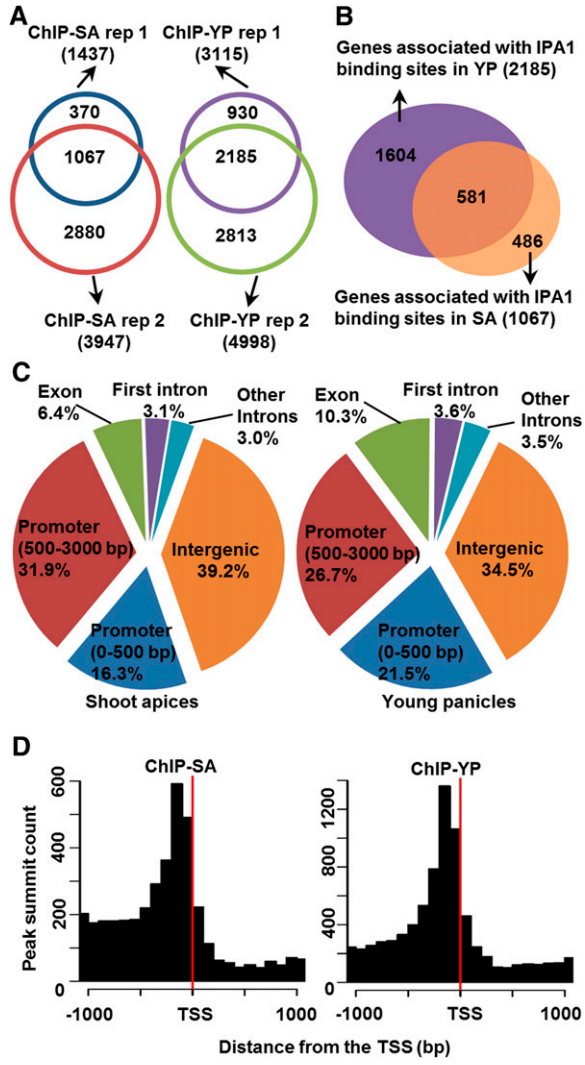

Figure 2. IPA1 Binding Sites in Rice Genome.

(A) Overview of genes associated with IPA1 binding sites in four IPA1 ChIP-seq results. rep, replicate.

(B) Genes reproducibly associated with IPA1 binding sites in YPs or SAs.

(C) Distribution of IPA1 binding peaks in rice genome.

(D) IPA1 binding peaks highly enriched in the −500 to 0 bp of promoter regions in both SAs and YPs. The overlapping peaks in SAs or YPs were used for analysis.

upstream from transcription start sites (TSSs), which accounted for ~48% of all the peaks in both SAs and YPs (Figure 2C). Besides the promoter region, the binding sites also showed similar genome distribution between two tissues except that the binding sites were increased in coding regions but decreased in intergenic regions in YP. To investigate the detailed IPA1 binding profile in the promoter region, the distance between each peak and its nearest gene was calculated. The histogram of these distances at the ±1-kb region around TSSs revealed that the IPA1 binding sites were strongly enriched in the promoter region, reaching the peak at ~200 bp upstream of TSSs (Figure 2D; see Supplemental Figure 5 online). Further comparison showed that the density of IPA1 binding sites was lower in the gene body regions than in the intergenic regions and much lower than in the promoter regions (see Supplemental Figure 5 online). All of these distribution patterns are consistent with the fact that IPA1 functions as a transcription factor.

Identification of IPA1 Binding Motifs

To investigate the IPA1 binding motifs, the ±50-bp flanking sequences around the peak summits were masked by RepeatMasker and then submitted to the motif searching program Discriminative Regular Expression Motif Elicitation (Bailey, 2011) to calculate the statistically overrepresented motifs. Three motifs were found (Figure 3A; see Supplemental Figure 6 online). Among them, the first showed the most conserved sequence GTAC, while the second and third ones were similar to each other and could be combined as one motif TGGGCC/T. Therefore, the motifs GTAC and TGGGCC/T were used for further analysis. By examining the density plots of motifs within all peaks and comparison to the randomly chosen motif GATC, the GTAC motifs were found to show strong enrichment precisely in the peak summits and to decrease to the background level at the flanking ±200-bp sites, while the TGGGCC/T motifs were mostly enriched 20 to 30 bp around the peak summits (Figure 3B; see Supplemental Figure 7 online). This indicates that although the two motifs are enriched around peak summits, different binding patterns exist between them. The identification of the GTAC motif is consistent with the previous finding that IPA1 could directly bind to the GTAC core sequence (Figure 1C). However, through the EMSA assay, IPA1 did not show direct binding affinity to the probe containing the TGGGCC/T motif (Figure 3C), indicating that TGGGCC/T is an indirect binding motif and may be bound by IPA1-interacting proteins.

To study the features of these two motifs, we established a quantitative method based on naïve Bayesian classifier and boosting algorithm (Jansen et al., 2003; Rhodes et al., 2005), which determines the log likelihood ratio (LLR) of whether the motifs in the peak are functional according to the findings that the motifs located near the peak summits are more likely to be functional (see Supplemental Figure 8 online). We obtained an LLR for the GTAC motif and one for the TGGGCC/T motif for every peak (see Supplemental Figure 9 online). A proof-of-concept analysis showed that both LLRs were well correlated with the binding affinity of peaks measured by the height of peak summits, and the LLR scores of both motifs were also higher in overlapping peaks than nonoverlapping peaks (see Supplemental Figure 10 online). Both results indicated that the LLR scores could distinguish the functional motifs in peaks.

We then examined whether the two motifs co-occur in the same peaks. For each motif, peaks were divided into six levels. The first level was those peaks with no motif sequences within them, and all other peaks were divided into five levels based on the LLR values. The number of peaks with different LLR levels for two motifs was counted (Figure 3D; see Supplemental Figure 11 online), and the results showed that these two motifs tended to appear in different peaks. Comparison of the genome distribution of peaks with different LLR levels for the two motifs revealed an opposite trend of genome locations. The percentage of peaks located in the promoter regions was correlated with LLR levels of the TGGGCC/T motif in both tissues, while the GTAC motif showed the opposite trend (Figures 3E and 3F; see Supplemental Figure 12 online). However, the detailed peak profile near the TSS region showed that the GTAC peaks were still enriched in promoters (empirical P value < 0.01), although not as markedly as the TGGGCC/T peaks (see Supplemental Figure 13 online). These results exclude the possibility that statistical overrepresentation of TGGGCC/T in IPA1 ChIP-seq was due to the colocalization with GTAC in the genome.

IPA1 Binds to the TGGGCC/T Motif through Interacting with PCF1 and PCF2

The motif TGGGCC/T was previously reported as a *cis*-element in the promoter of the gene encoding a proliferating cell nuclear antigen, an important factor in the cell cycle (Kosugi and Ohashi, 1997), and targeted by PCF1 and PCF2, two members of the TCP family that contains TB1 and CYCLOIDEA (CYC) (Kosugi and Ohashi, 1997; Guo et al., 2007). Since IPA1 is unable to directly bind the TGGGCC/T motif (Figure 3C), it is possible that IPA1 targets the TGGGCC/T motif through its interaction with PCF1 or PCF2. We therefore performed yeast two-hybrid assays to test this hypothesis and found that IPA1 could interact with both PCF1 and PCF2, but not with TCP3 (Figure 4A). The interactions were further confirmed by bimolecular fluorescence complementation (BiFC) assays in rice protoplasts (Figure 4B). These results demonstrated that PCF1 and PCF2 could act as mediators of the association between IPA1 and TGGGCC/T. We then tested whether IPA1 could target the TGGGCC/T motif through interaction with PCF1 or PCF2 in an EMSA assay. Consistent with previous report, PCF1 and PCF2 were found to bind the TGGGCC/T motif and retard the probe motilities (see Supplemental Figures 14A and 14B online). In addition, a super shift band was also found, which is consistent with the fact that PCF1 and PCF2 can form homodimers (Kosugi and Ohashi, 1997). When the His-IPA1 fusion protein was added to the system, the super shift bands, which may contain both homodimers of GST-PCF1 or GST-PCF2 and heterodimers consisting of His-IPA1 and GST-PCF1 or GST-PCF2, were clearly enhanced (see Supplemental Figures 14A and 14B online). This demonstrates that IPA1 can target the TGGGCC/T motif through interaction with PCF1 and PCF2. Further confirmation was obtained from ChIP-qPCR assays using *ProAct:PCF1-GFP* and *ProAct:PCF2-GFP* transgenic calli. The selected regions enriched with the TGGGCC/T motif in IPA1 ChIP-seq were also

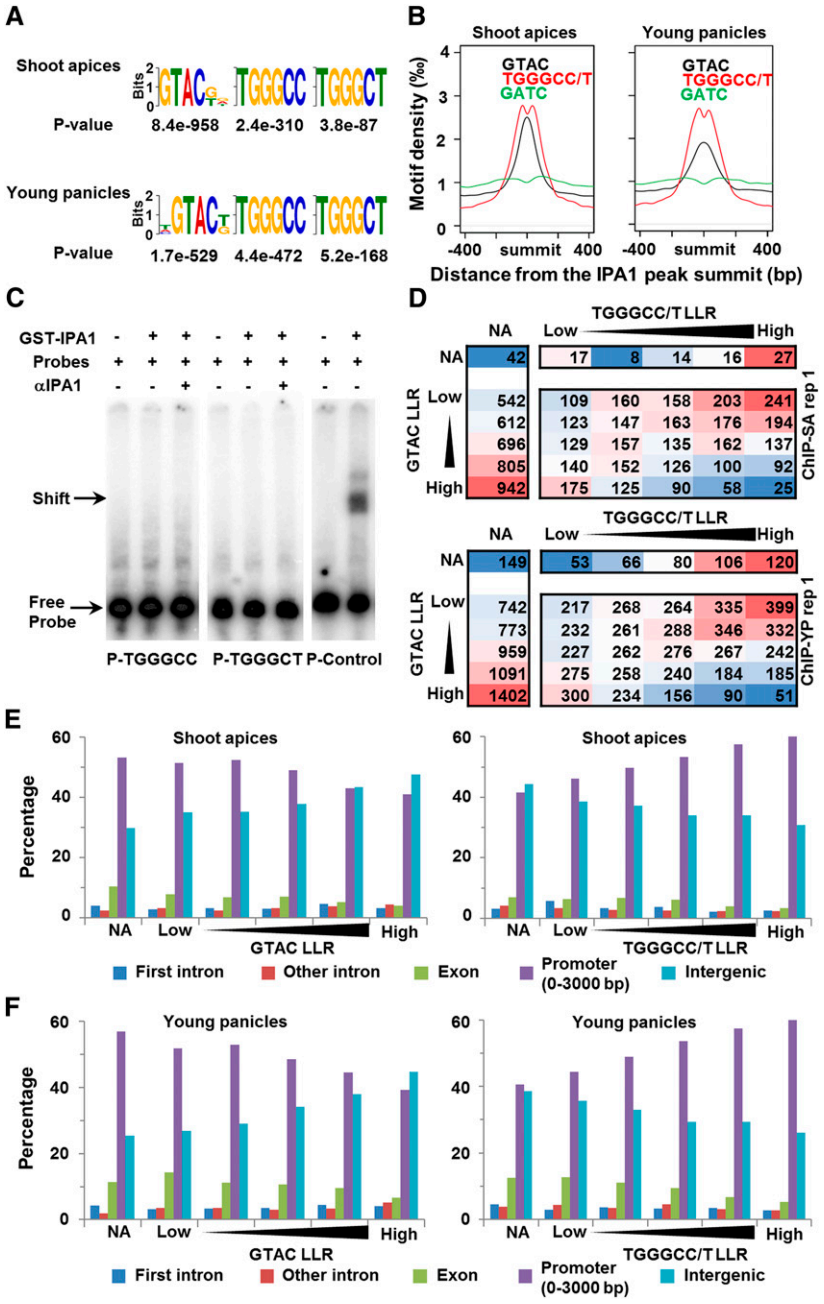

Figure 3. Binding Motifs Identified by ChIP-Seq.

(A) Binding motifs identified in the IPA1 overlapping binding peaks in SAs and YPs.

(B) Density plots of different IPA1 binding motifs around the summits of overlapping peaks in SAs and YPs. A nonrelated motif (GATC) was used as a negative control.

(C) No detectable binding of GST-IPA1 to TGGGCC/T, revealed by unchanged electrophoretic mobility of probes with the TGGGCC/T motif at the presence of GST-IPA1. P-Control, the positive control probe containing the GTAC motif.

(D) Two binding motifs showing the opposite distribution trends in IPA1 binding peaks in ChIP-SA rep 1 and ChIP-YP rep 1. The peaks with GTAC or TGGGCC/T were divided into five equal groups based on the LLR values for each motif. Autoscaled blue-red heat map was used to show peak counts in each separate matrix. NA, not applicable (no such motif); rep, replicate.

(E) and **(F)** Distribution of the peaks divided by the LLR of GTAC or TGGGCC/T in ChIP-SA rep 1 **(E)** and ChIP-YP rep 1 **(F)**. The peaks with GTAC or TGGGCC/T were divided into five equal groups based on the LLR values for each motif.

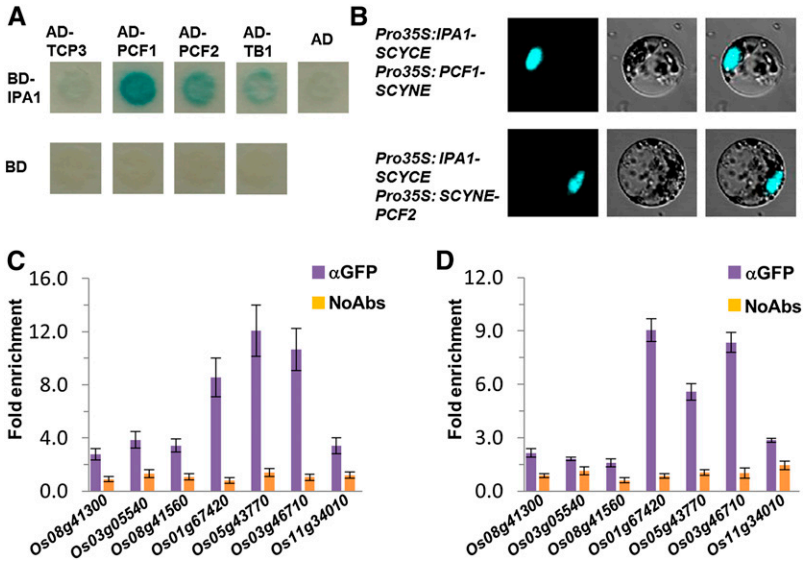

Figure 4. IPA1 Targets TGGGCC/T Motif through Interaction with PCF1 and PCF2.

(A) IPA1 interacts with PCF1, PCF2, and Os TB1 in a yeast-two hybrid assay. IPA1 was fused to the GAL4 binding domain (BD); PCF1, PCF2, Os TB1, or TCP3 was fused to the GAL4 activation domain (AD).

(B) IPA1 interacts with PCF1 or PCF2 in a BiFC assay. IPA1 was fused to the N-terminal region of cyan fluorescent protein. PCF1 or PCF2 was fused to the C-terminal region of cyan fluorescent protein.

(C) and **(D)** Examples of IPA1 binding regions bound by PCF1 **(C)** or PCF2 **(D)** in a ChIP assay. All primers were designed based on the peak sequences enriched in IPA1 ChIP-seq. The fold enrichment was normalized against the promoter of *Ubiquitin*. Values are means ± SE (n = 3).

enriched by PCF1 and PCF2 (Figures 4C and 4D). Taking all of these findings together, we conclude that IPA1 can target the TGGGCC/T motif through interacting with PCF1 and PCF2.

Genes Associated with IPA1 Binding Sites Enriched in Plant Development Pathways

To further study how IPA1 influences plant architecture, functional analysis of genes associated with IPA1 binding sites was performed, revealing that IPA1 could regulate different pathways that affect plant growth and development (Figure 5A). A plant ontology analysis revealed that IPA1 could bind to the promoters of genes that are expressed in cardinal organs in both SAs and YPs, but bind to genes expressed in anthers, gynoeciums, and stamens only in YPs (Figure 5A). For growth stage ontology (GRO), only in YPs could IPA1 bind to the genes that are expressed at the mature grain growth and embryo development stages, including GRO:0007045 (09-mature grain stage) and GRO:0007175 (embryo stage EM8) (Figure 5A). The number of genes associated with IPA1 binding sites was greatly increased in YP, and these genes were likely to be responsible for embryo development. For environment ontology (EO), a strong enrichment gene set, EO:0007200 (short-daylength regimen), was found, which is consistent with the fact that *IPA1* affects the flowering time in transgenic lines (see Supplemental Figure 15 online) and the findings that IPA1 targets the promoters of *MADS56* and *FT LIKE1* (*FTL1*) (see Supplemental Figure 16 online). Further studies revealed that the TGGGCC/T-containing target genes were enriched mainly in development-related pathways (see Supplemental Figure 17 online).

Manual examination of literature relevant to genes associated with IPA1 binding sites identified 28 important plant architecture-related genes (Table 1), which could be classified into several functional categories, including transcription factors, plant hormone–related genes, enzymes, and transcriptional regulators. The promoters of these important rice architecture regulators, such as *DEP1*, *LOG*, *SLR1*, *PIN1b*, and Os *TB1*, were found to be bound by IPA1. EMSA assays confirmed that IPA1 could directly target the promoter or first intron of *LOG*, *SLR1*, and *PIN1b* (see Supplemental Figure 18 online), suggesting that these genes may be the targets of IPA1 in regulating plant architecture.

Expression Profile of Genes Associated with IPA1 Binding Sites

To further study how IPA1 regulates the expression of the genes associated with IPA1 binding sites, RNA-seq was performed with SAs and YPs of NEAR ISOGENIC LINEs (NIL-*ipa1* and NIL-*IPA1*) plants with two biological replicates. A total of 3979 and 1628 differentially expressed genes were found in SAs and YPs, respectively (P value < 0.05) (see Supplemental Data Sets 1C and 1D online). Among these differentially expressed genes, there were ~10% of the genes associated with IPA1 binding sites. Of those, 47 and 46 genes associated with IPA1 binding sites were significantly downregulated in SAs and YPs, whereas 79 and 143 were significantly upregulated in both tissues (Table 2). To check the effect of IPA1 on the genes with different motifs in their promoters, we further grouped these genes based on the motif types of the peaks located on their promoters. In SAs,

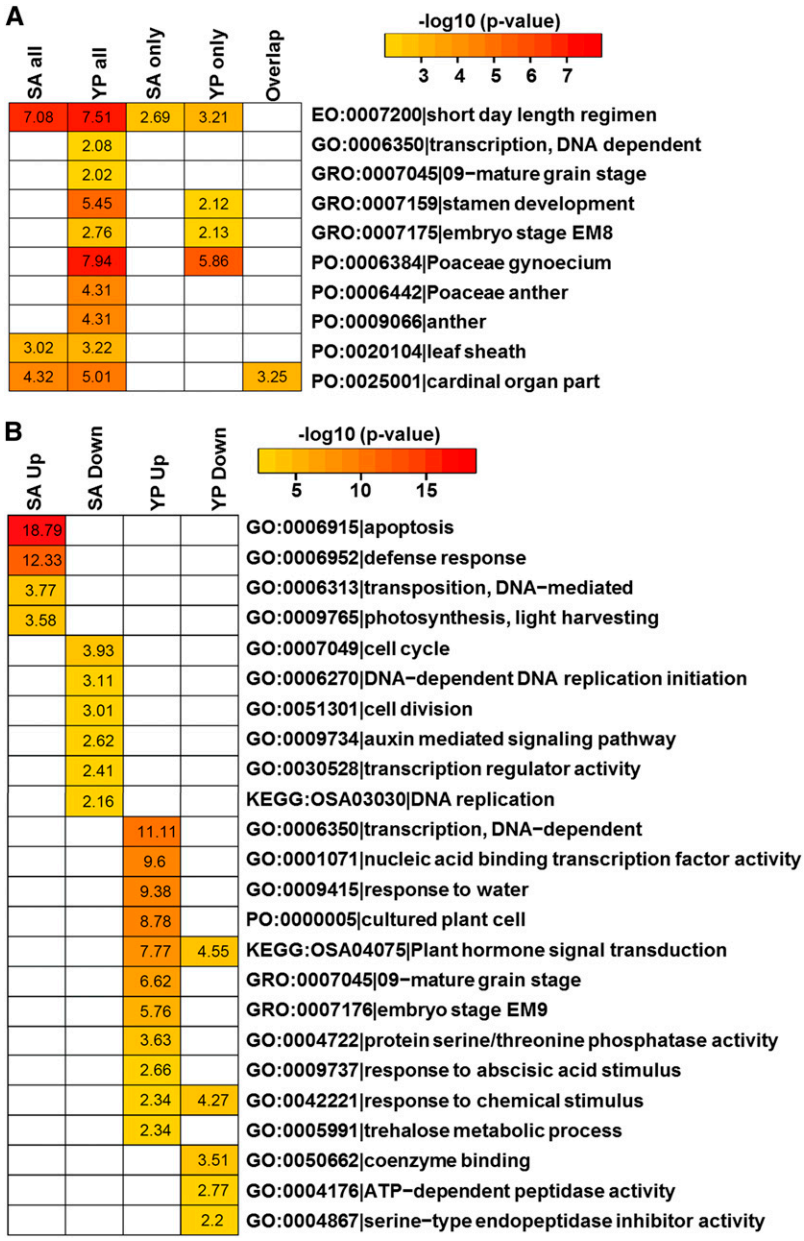

Figure 5. Enriched Pathways of Genes Associated with IPA1 Binding Sites and Differentially Expressed Genes Revealed by RNA-Seq.

Enriched pathways of genes associated with IPA1 binding sites **(A)** and differentially expressed genes revealed by RNA-seq **(B)**. The number in each cell indicates -log10 (P values) of the pathway enrichment tested by Fisher's exact test with Bonferroni correction and a blank cell indicates no significance. SA all, all the genes associated with IPA1 binding sites in SAs; YP all, all the genes associated with IPA1 binding sites in YPs; SA only, genes associated with IPA1 binding sites specifically in SA; YP only, genes associated with IPA1 binding sites specifically in YP; Overlap, genes associated with IPA1 binding sites both in SAs and YPs; SA Up, upregulated genes in *ipa1* SA; SA Down, downregulated genes in *ipa1* SA; YP Up, upregulated genes in *ipa1* YPs; YP Down, downregulated genes in *ipa1* YPs; GO, gene ontology; PO, plant ontology.

13 genes with the TGGGCC/T motif in their promoters were upregulated and 12 downregulated, while 24 genes with GTAC were upregulated and 8 downregulated (Table 2). In YPs, 37 genes with TGGGCC/T motif in their promoters were upregulated and seven downregulated, while 24 genes with GTAC were upregulated and 14 downregulated (Table 2).

Further analysis of the differentially expressed genes in RNA-seq data showed that the upregulated genes in SA are mainly enriched in the pathways related to apoptosis, defense response, and photosynthesis, while the downregulated genes are enriched in pathways related to cell cycling and auxin signaling (Figure 5B). In YPs, the upregulated genes were mainly enriched

Table 1. Functional Categories of Genes Associated with IPA1 Binding Sites

		Locations of IPA1 Binding Sites[a]	
Gene ID	Annotation	SAs	YPs
Transcription Factors			
LOC_Os03g49990	SLR1	P	P
LOC_Os07g39480	WRKY78	P	P
LOC_Os01g38530	EF3	N	P
LOC_Os06g06750	MADS5	N	I
LOC_Os08g41950	MADS7	N	P, I
LOC_Os02g52340	MADS22	N	P
LOC_Os03g49880	TB1	N	P
LOC_Os01g68370	VP1	N	P
LOC_Os07g25710	PHR2	N	P
Plant Hormone–Related Genes			
LOC_Os02g36974	GID2	N	P
LOC_Os06g15620	GSR1	N	P
LOC_Os05g40384	EUI1	I	I
LOC_Os01g40630	LOG	N	P, I
LOC_Os02g50960	PIN1b	N	P
LOC_Os01g49000	DGL1	N	P
Enzymes			
LOC_Os11g09280	PDIL1-1	P	P
LOC_Os01g67420	EG1 Like	N	P
LOC_Os06g24730	NYC3	N	P
LOC_Os09g12660	APS1	N	P
LOC_Os08g25734	APS2	N	I
Transcriptional Regulators			
LOC_Os02g04160	TEF1	P	P
LOC_Os08g06480	REL2	P	N
Others			
LOC_Os05g03430	SIZ1	P	P
LOC_Os03g11900	MST4	P	N
LOC_Os12g36030	PMS3	N	P, I
LOC_Os09g26999	DEP1	N	P
LOC_Os09g27060	DDM1a	N	P
LOC_Os12g17080	OGR1	N	P

[a]P, promoter; I, first intron; N, no binding sites.

in development-related pathways and response to abiotic stresses, while the downregulated genes affected mainly coenzyme binding, Ser-type endopeptidase inhibitor activity and ATP-dependent peptidase activity (Figure 5B). In addition, several development-related pathways showed significant enrichment in genes associated with IPA1 binding sites, which suggests that the development-related genes may play important roles in the formation of panicle morphology in *ipa1*. In addition, the genes related to plant hormone signaling and response to chemical stimuli were affected in both down- and upregulated manners, indicating IPA1 may also affect the panicle phenotype through those two pathways (Figure 5B).

IPA1 Suppresses Rice Tillering Mainly through Positive Regulation of Os *TB1*

To understand how IPA1 regulates shoot branching, we focused on Os *TB1* based on the facts that Os *TB1* acts as a negative regulator of rice tillering (Takeda et al., 2003; Minakuchi et al., 2010) and that Os *TB1* is a potential direct target of IPA1 (Table 1). The peak summits for IPA1 binding sites were located 96 and 187 bp upstream of the Os *TB1* TSS in the two YP replicates, respectively (Figure 6A; see Supplemental Figure 19 online). However, the Os *TB1* promoter was significantly enriched in both SAs and YPs by the ChIP-qPCR analysis, indicating that Os *TB1* is probably under the control of IPA1 in both tissues (Figure 6B). Further analysis of binding peaks revealed that the GTAC motif, rather than the TGGGCC/T motif, existed in the Os *TB1* promoter. To test whether IPA1 can directly bind to the GTAC motif in the Os *TB1* promoter, we performed an EMSA assay and found that GST-IPA1 could bind to a 59-bp probe from the Os *TB1* promoter (Figure 6C; see Supplemental Figure 20 online). The mutation of GTAC to ATAC abolished its binding affinity, demonstrating that the binding was dependent on the GTAC motif.

As a negative regulator in rice tiller development, Os *TB1* is expressed in axillary buds, and its deficiency results in a semi-dwarf phenotype with a significant increase in tiller number (Takeda et al., 2003; Minakuchi et al., 2010). This suggests that the reduced tiller phenotype of *ipa1* plants may result from the

Table 2. Genes Associated with IPA1 Binding Sites or with a Significant Expression Level Change in SAs and YPs of the *ipa1* Mutant

Genes Associated with IPA1 Binding Sites	Gene No.	Upregulated	Downregulated
In SAs			
All	1067	79	47
GTAC motif[a]	224	24	8
TGGGCC/T motif[b]	360	13	12
Both motifs	61	1	2
Others	422	41	25
In YPs			
All	2185	143	46
GTAC motif[a]	377	24	14
TGGGCC/T motif[b]	925	37	7
Both motifs	109	3	0
Others	774	79	25

[a]Genes that contain only the GTAC motif.
[b]Genes that contain only the TGGGCC/T motif.

direct activation of Os *TB1* by *IPA1*. The RNA level of Os *TB1* was significantly upregulated in SAs in *NIL-ipa1*, but much less significantly in YPs (Figure 6 D). Furthermore, the double mutant analysis showed that the mutation of Os *TB1* could suppress the tillering phenotype of *ipa1* (Figure 6E).

Since Os TB1 is homologous to PCF1 and PCF2, we tested whether Os TB1 could also interact with IPA1. A weak interaction was detected in the yeast two-hybrid assay (Figure 4A), and EMSA further showed that Os TB1 could directly bind the TGGGCC/T motif (see Supplemental Figure 21 online),

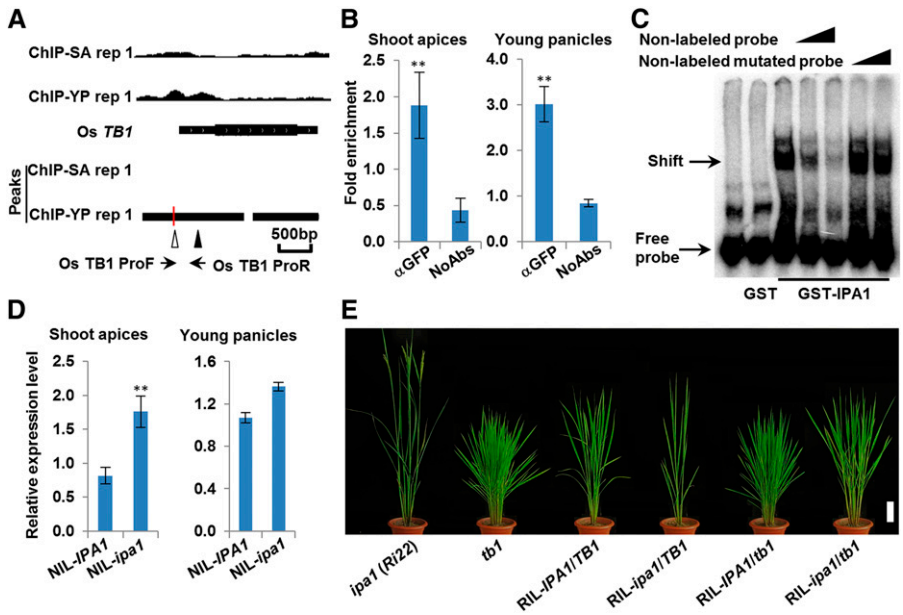

Figure 6. *IPA1* Directly and Positively Regulates the Expression of Os *TB1*.

(A) IPA1 binding profile in the promoter of Os *TB1*. The open arrowhead refers to the GTAC around the peak summit and the solid arrowhead to the GTAC around the subsummit. The red vertical line denotes the peak summit. The primer pair Os *TB1 Pro* (see Supplemental Table 1 online) was used for amplifying the Os *TB1* promoter.

(B) Validation of IPA1 direct binding sites in the Os *TB1* promoter by ChIP-qPCR analysis. The fold enrichment was normalized against the promoter of *Ubiquitin*. αGFP, antibodies against GFP. Values are means ± SE (n = 3). The double asterisks represent significant difference determined by the Student's t test at $P < 0.01$.

(C) EMSA showing that GST-IPA1 could directly bind to the promoter of Os *TB1*. The 10- and 40-fold excess nonlabeled or mutated probes were used for competition.

(D) Comparison of Os *TB1* expression levels between NIL-*IPA1* and NIL-*ipa1* in SAs and YPs, respectively. Rice *Actin* was used as reference. Values are means ± SE (n = 3). The double asterisks represent significant difference determined by the Student's t test at $P < 0.01$.

(E) Suppression of tiller number by *tb1/fc1* in RIL-*ipa1*/*tb1* lines. Bar = 20 cm.

indicating that Os TB1 also functions as an adaptor for the interaction between IPA1 and the TGGGCC/T motif. Considering that Os TB1 is not only a target of IPA1, but also can interact with IPA1, we propose that Os TB1 is probably involved in the feedback regulation of IPA1 transcriptional activity.

IPA1 Regulates Panicle Length and Plant Height through *DEP1*

DEP1 is another important regulatory gene that affects rice architecture, especially panicle morphology. A truncated mutation of DEP1 enhances panicle meristematic activity, resulting in reduced length of inflorescence internodes, increased number of grains per panicle, and a consequent increase in grain yield (Huang et al., 2009). IPA1 ChIP-seq analysis revealed that *DEP1* was also a direct target of IPA1 (Table 1). The peak summits of IPA1 binding were located 566, 514, 440, and 500 bp upstream of the *DEP1* TSS in SA rep 1, SA rep 2, YP rep 1, and YP rep 2, respectively (Figure 7A; see Supplemental Figure 22 online). Within the peaks in the *DEP1* promoter, besides the highest peak summit, there are other two subsummits showing local max sequencing reads (Figure 7A; see Supplemental Figure 22 online). Through analyzing the *DEP1* promoter sequence, several GTAC motifs were found, and three sites around the peak summits and subsummits were considered to be responsible for the binding of IPA1. To confirm this, ChIP-qPCR was performed. As shown in Figure 7B, the two specific regions were significantly enriched. We then tested whether IPA1 could directly bind to the promoter of *DEP1* by EMSA with three 59-bp sequences around the peak summit and subsummits as probes and found that IPA1 could bind to all the three probes but could not bind to a probe containing the mutated binding core motif (Figure 7C; see Supplemental Figure 23 online). These results demonstrate that IPA1 can directly bind to the promoter of *DEP1* at different sites and the GTAC core motifs are responsible for IPA1 binding, suggesting that *DEP1* is a direct target of IPA1.

To further understand the biological functions of *DEP1* as a direct target of *IPA1*, we generated recombinant inbred lines by crossing *Ri22*, an *ipa1*-carrying cultivar (Jiao et al., 2010), with *LJ5*, a rice variety carrying the *dep1* mutation (Huang et al., 2009). As shown in Figures 8A and 8B, the plant height of the RIL-*ipa1*/*dep1* lines was reduced to a similar level to the RIL-*IPA1*/*dep1* lines. Consistent with the previous result that *dep1* does not affect rice tillering, the tiller number of RIL-*ipa1*/*dep1* lines exhibited no significant difference from RIL-*ipa1*/*DEP1* lines (see Supplemental Figure 24A online). We also noticed that the panicle morphology of the RIL-*ipa1*/*dep1* lines was dense and erect (Figures 8C and 8D). Compared with the RIL-*ipa1*/*DEP1* lines, the panicle length of RIL-*ipa1*/*dep1* lines was significantly reduced, but no obvious change in panicle branches was found (see Supplemental Figures 24B and 24C online). Like *IPA1*, *DEP1* was also strongly expressed in culms, SAs, and YPs, but weakly in roots (Figure 8E), suggesting that *IPA1* may regulate the expression of *DEP1*. We further examined the expression of *DEP1* in NIL-*ipa1* lines and found that *DEP1* transcripts were significantly increased in the SA of NIL-*ipa1* lines, but only slightly in YP (Figure 8F). Therefore, it is likely that *IPA1* functions as a positive regulator of DEP1 in regulating plant height and panicle length in rice.

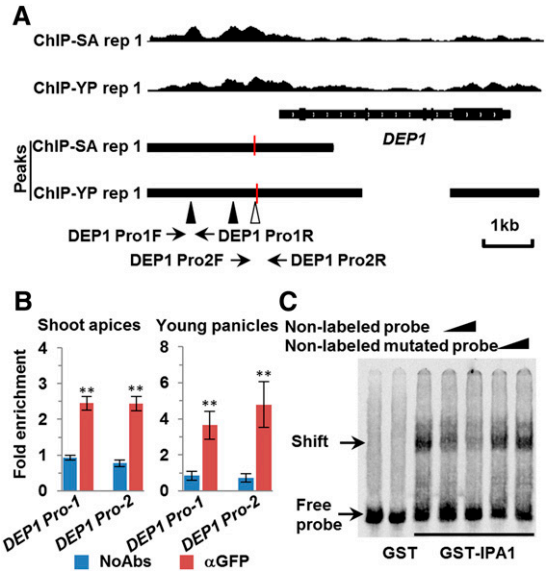

Figure 7. IPA1 Directly Binds to the *DEP1* Promoter.

(A) IPA1 binding profile in the promoter of *DEP1*. The open arrowhead refers to the GTAC around the peak summit, solid arrowheads to other GTAC sequences around subsummits, and red vertical lines to peak summits. Primer pairs *DEP1-Pro1* and *DEP1-Pro2* (see Supplemental Table 1 online) were used for amplifying *DEP1 Pro-1* and *DEP1 pro-2*, respectively.

(B) Validation of IPA1 direct binding sites in the *DEP1* promoter by ChIP-qPCR analysis. The fold enrichment was normalized against the promoter of *Ubiquitin*. αGFP, antibodies against GFP. Values are means ± SE ($n = 3$). The double asterisks represent significance difference determined by the Student's *t* test at $P < 0.01$.

(C) Direct binding of IPA1 to the *DEP1* promoter in EMSA. The 10- and 40-fold excess nonlabeled or mutated probes were used for competition.

DISCUSSION

Genome-wide identification of target genes contributes greatly to determining the functions and molecular mechanisms of transcription factors. IPA1 is a recently identified key transcription factor that regulates rice plant architecture. Here, we present a genome-wide identification of direct IPA1 target genes that regulate rice development using a ChIP-seq approach, which will enrich our understanding of the molecular basis of ideal plant architecture.

A Complex Genetic Network Mediated by IPA1

IPA1 is a pleiotropic gene and plays an intricate role in rice plant architecture (Jiao et al., 2010). In this study, we identified global genes associated with IPA1 binding sites using a ChIP-seq approach in SA and YP to investigate the diversity of regulation at different developmental stages. Our results provide several insights into the genetic network regulating rice plant architecture. First, genes associated with IPA1 binding sites largely overlap between SAs and YPs. Many more genes are associated with IPA1 binding sites in YPs and several extra pathways in flower and embryo development are shown in YPs (Figure 5A).

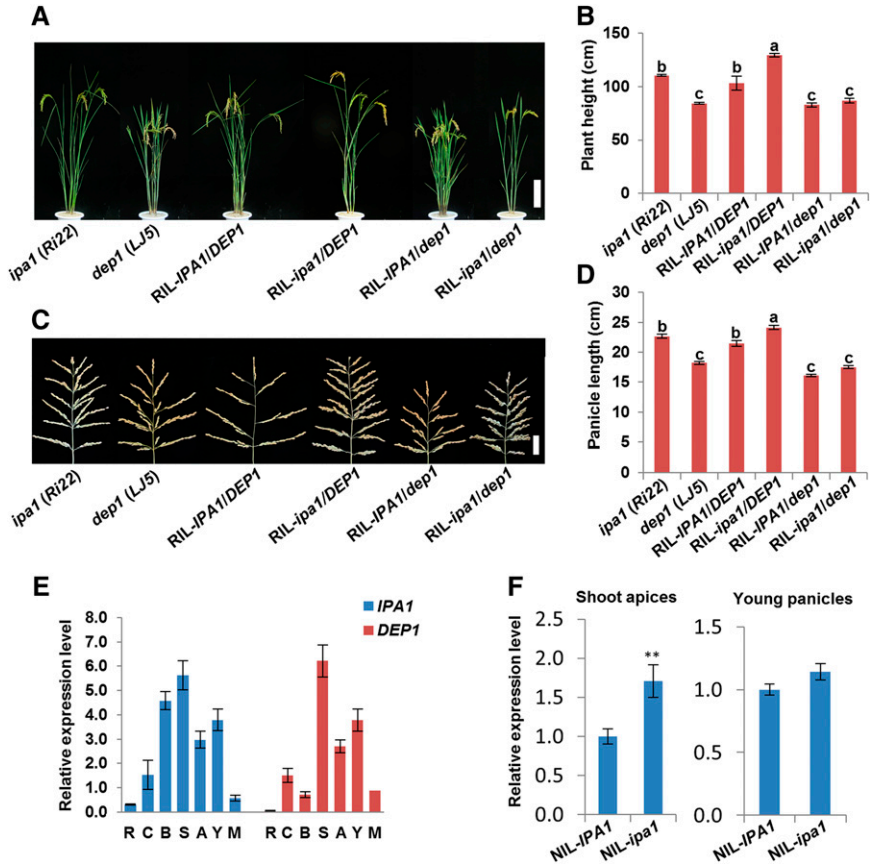

Figure 8. *DEP1* Is Positively Regulated by *IPA1*.

(A) Suppression of plant height by *dep1* in RIL-*ipa1*/*dep1* lines. Bar = 20 cm.

(B) Statistical analysis of **(A)**. Values are means ± SE (n = 15). Different lowercase letters indicate significant differences between different genotypes ($P < 0.01$, one-way analysis of variance).

(C) Suppression of panicle length by *dep1* in RIL-*ipa1*/*dep1* lines. Bar = 5 cm.

(D) Statistical analysis of **(C)**. Values are means ± SE (n = 15). Different lowercase letters indicate significant differences among different genotypes ($P < 0.01$, one-way analysis of variance).

(E) Expression patterns of *IPA1* and *DEP1* in different tissues revealed by qPCR analyses. R, roots; C, culms; B, leaf blades; S, leaf sheathes; A, SAs; Y, YPs; M, mature panicles. Rice *Ubiquitin* was used as reference. Values are means ± SE (n = 3).

(F) Comparison of *DEP1* expression levels between NIL-*IPA1* and NIL-*ipa1* in SAs and YPs, respectively. Rice *Actin* was used as reference. Values are means ± SE (n = 3). The double asterisks represent significant difference determined by the Student's t test at $P < 0.01$.

These results suggest that the binding patterns may be altered during rice development such that IPA1 gradually binds to new target genes as development progresses. This could be caused by gradually opened chromatin structure during plant development (Li et al., 2002; Reyes et al., 2002), in which the potential IPA1 target genes of the next development stage are released from the dense chromatin structure and make their promoters accessible for IPA1 binding.

Second, the expression levels of genes involved in response to environment and in abscisic acid signaling were changed significantly in *ipa1* (Figure 5B), indicating that IPA1 may affect the stress response. Our results also show that IPA1 significantly affects plant hormone signaling with both up- and downregulation of downstream genes. In addition, we found that IPA1 can directly bind to the promoters of Os *TB1*, *PIN1b*, *SLR*, and *LOG*, which are important components in plant hormone pathways. All of these results suggest that plant hormones play key roles in the *IPA*-mediated regulation network of plant architecture (Figure 9).

Third, IPA1 can target two types of motifs, a conserved GTAC motif and a novel TGGGCC/T motif. However, the TGGGCC/T motif is not directly bound by IPA1 (Figure 3); instead, it is likely to function as an indirect binding motif. It appears that IPA1 targets the TGGGCC/T motif through interaction with PCF1 and PCF2 (Figure 4; see Supplemental Figure 14 online). Our results also show that these two types of motifs tend to appear in different peaks. It is possible that IPA1 directly binds to key regulators, such as *DEP1* and Os *TB1*, which contain the GTAC motif and regulate the downstream genes in different biological pathways. At the same time, together with TCP proteins, such

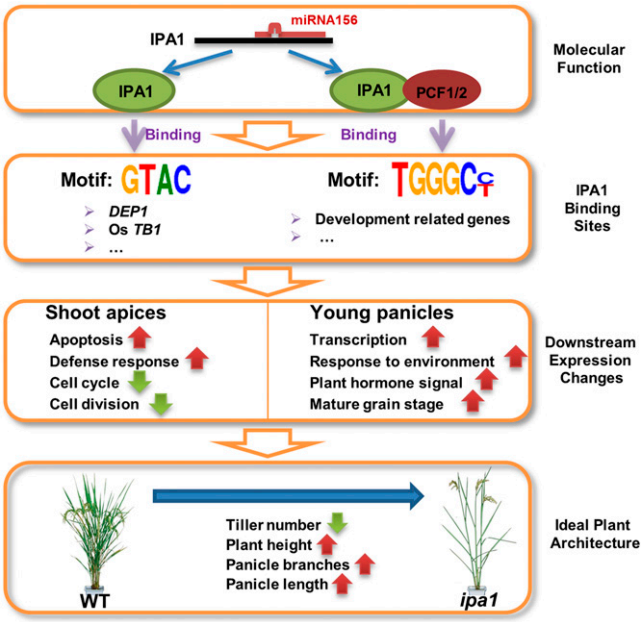

Figure 9. A Model for Rice Plant Architecture Regulation by *IPA1*.

IPA1 directly binds to the GTAC motif to regulate key plant architecture regulators, including *DEP1* and Os *TB1*, whereas it indirectly binds to the TGGGCC/T motif through interaction with PCF1 and PCF2 to modulate development-related genes. Consequently, the expression levels of genes involved in multiple biological processes, such as apoptosis, cell cycle, development, stress response, and plant hormone signaling, are altered, thus leading to the formation of ideal plant architecture.

as *PCF1* and *PCF2*, *IPA1* may also regulate a large number of development-related target genes that contain the TGGGCC/T motif in their promoters (Figure 9).

The TCP proteins are divided into Class I (also known as PCF or TCP-P class) and Class II (also known as CYC/TB1 or TCP-C class) subgroups based on their DNA binding domain sequences (Martín-Trillo and Cubas, 2010). Class I genes are widely expressed during plant development and mainly promote plant growth and proliferation, whereas class II genes are tightly regulated at multiple levels and prevent plant growth and proliferation (Martín-Trillo and Cubas, 2010). PCF1 and PCF2 (members of TCP-P class) can interact with IPA1 and act as mediators for IPA1 binding the TGGGCC/T motif. Moreover, IPA1 binds to the Os *TB1* (a member of the TCP-C class) promoter and has weak interaction with Os TB1 (Figures 4A and 6A to 6C), suggesting feedback regulation of Os TB1 on the transcriptional activity of IPA1. The different binding abilities of the two class TCP members to IPA1 or the promoters of downstream targets may provide more flexibility for IPA1 to regulate rice development. Upregulation of *TCP-C* genes may promote their interaction with IPA1, which in turn could mediate further regulation by IPA1 of *TCP-C* target genes. Alternatively, accumulation *TCP-C* genes may enable them to compete with *TCP-P* genes for binding to the target genes or interaction with their common partners. Further investigation of IPA1 in modulating the genetic cascades mediated by different TCP genes may promote our understanding of the roles of IPA1 in developmental processes beyond plant architecture (Figure 9).

SPL Genes Also Affect Phase Transition in Monocotyledons

IPA1 belongs to the *SPL* gene family and is the ortholog of *SPL9* from *Arabidopsis*. *SPL9* and its homologs are considered to act redundantly in phase transition. Most of the *SPL* genes are direct targets of miRNA156 and overexpression of miRNA156 precursors can downregulate the RNA level of *SPL* genes and substantially prolong the juvenile phase (Fornara and Coupland, 2009). *SPL9* directly binds to the promoters of *SOC1*, *AGL42*, and *FT* (Fornara and Coupland, 2009; Wang et al., 2009; Wu et al., 2009). In rice, *IPA1* is also targeted by miRNA156 and the heading date of *IPA1*-overexpressing transgenic lines is delayed (see Supplemental Figure 15 online), suggesting that a conserved regulation network may exist in monocotyledonous plants. Consistent with this, the finding that the direct target genes of *IPA1* are highly enriched in the short-daylength regimen (EO:0007200) suggests participation of IPA1 in regulating the phase transition (Figure 5A). Although no peak is found in the 500 bp upstream of the TSS of *MADS56* or *FTL1*, the rice homologs of *SOC1* and *FT*, IPA1 binding sites are enriched ~2 kb upstream of these genes, which suggests that direct regulation of IPA1 may exist (see Supplemental Figure 16 online). In addition, IPA1 also binds to the promoter of many flower development–related genes (Table 1), including several MADS box genes (Kobayashi et al., 2012). Therefore, *SPL* genes also play important roles in the phase transition in monocotyledons.

Formation of Ideal Plant Architecture

The concept of ideal plant architecture or new plant type was proposed decades ago. However, the molecular basis of the formation of ideal plant architecture still remains to be elucidated. In this study, we show that IPA1 act as key regulator in a genetic regulatory network shaping rice plant architecture. Regulation of transcription factors on their target genes usually varies in the particular developmental or cellular contexts (Spitz and Furlong, 2012), and genes associated with IPA1 binding sites overlapping in SAs and YPs could be differently regulated. *DEP1* is an important component regulating plant height and panicle length. During vegetative growth, *IPA1* may continuously and positively regulate the expression of *DEP1* in SAs. On the other hand, IPA1 can also bind to the promoter of *DEP1* in YPs, whereas no significant change of the *DEP1* RNA transcripts was observed, indicating that the regulation of *DEP1* by IPA1 is more complex than expected. Moreover, it has been shown that *IPA1* can be targeted by miR156 and miR529, which are preferentially expressed in different tissues and developmental stages (Jeong et al., 2011), suggesting a developmental or cellular context-dependent regulation of *IPA1*. Therefore, dissecting the molecular mechanism underlying the IPA-mediated genetic network responses to different developmental contexts and environmental stimuli will enrich our understanding of molecular basis of ideal plant architecture.

Genetic and biochemical studies have revealed that Os *TB1* is directly regulated by IPA1 and involved in the regulation of rice

tillering. Recently, studies of Os *TB1* and its orthologs, including *BRC1* in *Arabidopsis*, *TB1* in sorghum (*Sorghum bicolor*), and *BRC1* in pea (*Pisum sativum*), have shown that Os *TB1* and its orthologs are likely to act as integrators in multiple pathways. The expression levels of Os *TB1* and its orthologs have been found to be regulated in response to different signals, such as cytokinins, strigolactones, and the red to far-red light ratio (Minakuchi et al., 2010; Dun et al., 2012; Niwa et al., 2013). Moreover, Os *TB1* and its orthologs have also been shown to interact with other proteins to modulate the expression of its downstream genes (Guo et al., 2013; Niwa et al., 2013). Further identification of the downstream genes of Os TB1 and elucidation of how IPA1 interacts with other pathways in the regulation of Os *TB1* will contribute to understanding the role of IPA1 in plant architecture and other development processes in rice.

METHODS

Plant Materials

Rice (*Oryza sativa*) ssp *japonica* Nipponbare, *ProIPA1:7mIPA1-GFP* transgenic lines, and mutants *Ri22*, *LJ5*, and *fc1* (all originating from *japonica*) were grown in either the greenhouse or experimental field of Institute of Genetics and Developmental Biology (Huang et al., 2009; Jiao et al., 2010; Minakuchi et al., 2010). *Ri22*, an *ipa1*-carrying cultivar, was crossed to a *dep1* mutant *LJ5* or *tb1*/*fc1* mutant, and heterozygous plants from the F2 progeny were selected for further generating various genotypic lines.

ChIP

The wild-type rice (Nipponbare) and its transgenic lines generated from the transformation of *ProIPA1:7mIPA1-GFP*, *ProAct:PCF1-GFP*, and *ProAct:PCF2-GFP* were used for ChIP assays according to the method described previously (Saleh et al., 2008) with some modifications. Briefly, 5 g of 1.5-cm SAs of 4-week-old seedlings or <2-cm YPs of adult plants grown in the field or transgenic calli were harvested. Samples were cross-linked with 1% (v/v) formaldehyde under vacuum for 8 min and then ground to powder in liquid nitrogen. The chromatin complexes were isolated and sonicated and then incubated with polyclonal anti-GFP antibodies (Abcam AB290). The precipitated DNA was recovered and dissolved in water and stored at –80°C for later use.

Construction of Illumina Sequencing Libraries and Sequencing of ChIP DNA

Illumina sequencing libraries were constructed with the above-prepared DNA samples mainly according to the manufacturer's instructions. The ends of DNA fragments were repaired and ligated to an adaptor. Then, DNA fragments of 270 to ~330 bp were recovered from the gel and amplified by PCR for 18 to 20 cycles. The amplified DNA products were collected, ligated to the pEASY-Blunt vector for a quality test, and then sequenced with Illumina system Genome Analyzer (ChIP-SA rep 1 and ChIP-YP rep 1) or Hiseq2500 (ChIP-SA rep 2 and ChIP-YP rep 2).

Analysis of ChIP-Seq Data

Sequencing reads from SAs and YPs for ChIP and input DNA were mapped to Release 6 of the Michigan State University Rice Genome (Ouyang et al., 2007) using SOAP2 (Li et al., 2009) with parameters -r 0 -n 0 -v 0 -l 75. Cross-correlation metrics were calculated using phantompeakqualtools (http://encodeproject.org/ENCODE/encodeTools.html#metrics) (Landt et al., 2012). Only uniquely mapped reads were used for peak identification, and IPA1 binding peaks were obtained by model-based analysis of ChIP-seq (Zhang et al., 2008) with default parameters. The peak summits were used to define the location types in the genome by the following criteria. If a peak summit was located in (1) a gene's first intron, (2) a gene's promoter region (upstream 3000 bp from the TSS), (3) a gene's exon, or (4) a gene's intron, it was labeled according to the first criterion it matched. Because of the detailed peak distribution on the genome and promoter region, a strict cutoff was used to identify IPA1 target genes by labeling the genes with peak summits located in the upstream 500 bp from the TSS or first introns. As for Zhang et al. (2013), the genes identified in both replicates were used for further analysis.

Motif Search and Classification

For all peaks present in two replicates, if a peak in one replicate overlapped with any peak in another replicate, it was labeled as an overlapping peak; otherwise, it was labeled as a nonoverlapping peak. One hundred base pairs around the top of the peak summits for all overlapping peaks (upstream 50 bp and downstream 50 bp) were filtered by RepeatMasker Web Server (http://www.repeatmasker.org), and then the masked sequences were subjected to Discriminative Regular Expression Motif Elicitation (Bailey, 2011). All loci matching GTAC and TGGGCC/T within each peak summit ±500 bp were identified. The densities of the loci of the two motifs were drawn using the density plot tool in R 3.0. The information that the motifs were densely distributed near peak summits was used to predict functional motifs from the random sequences that also matched the motif patterns, and a likelihood ratio score was addressed for each motif in each peak using the basic principle of naïve Bayesian classifier (Jansen et al., 2003; Rhodes et al., 2005). Details are given in Supplemental Methods 1 online.

Construction of Illumina Sequencing Libraries and Sequencing of RNA

Total RNAs were isolated from rice seedlings or YPs using a TRIzol kit (Invitrogen) according to the user manual. Illumina sequencing libraries were then constructed according to the manufacturer's instructions. The libraries were then sequenced with Illumina system Hiseq2500.

Analysis of RNA-Seq Data

Analysis of RNA-seq data followed the standard protocol described by Trapnell et al. (2012). The raw reads of RNA-seq were mapped to Release 6 of the Michigan State University Rice Genome (Ouyang et al., 2007) by Tophat (Trapnell et al., 2009). Cuffdiff (Trapnell et al., 2009, 2010) was used to calculate the fragments per kilobase of exon per million fragments mapped of each gene and identify the differentially expressed genes between NIL-*ipa1* and NIL-*IPA1* in SAs and YPs.

Ontology Analysis

Ontology data sets and their structure files, including gene ontology (Ashburner et al., 2000), plant ontology (Avraham et al., 2008), growth ontology (Pujar et al., 2006), trait ontology (Jaiswal et al., 2002), and environment ontology, were collected from the Gramene database (Youens-Clark et al., 2011). These data sets were then propagated from the leaf nodes to its parent nodes in ontology structure using the published method (Yu, H. et al., 2010). Kyoto Encyclopedia of Genes and Genomes (KEGG) pathway information was collected from the KEGG database (Kanehisa et al., 2012).The enriched functions of genes associated with IPA1 binding sites and differentially expressed genes in RNA-seq data sets were determined with these ontology data sets and KEGG pathways using Fisher's exact test with Bonferroni correction.

ChIP-qPCR

The prepared DNA in ChIP was applied for qPCR using respective primer pairs (see Supplemental Table 1 online) in an EVER Green PCR Master Mix (Bio-Rad) with a Bio-Rad CFX96 real-time PCR detection system. PCR reactions were performed in triplicate for each sample, and the expression levels were normalized to the input sample for enrichment detection. The fold enrichment was calculated against the *Ubiquitin* promoter. No addition of antibodies (NoAbs) was served as a negative control.

Transcriptional Activity Assay in Rice Protoplasts

To generate the GAL4BD-IPA1 construct, the full-length *IPA1* cDNAs were amplified by the primer sets listed in Supplemental Table 2 online and cloned into the *Xba*I and *Kpn*I sites of the GAL4-BD vector. The plasmids containing GAL4BD-IPA1, 35sLUC, and pRTL were introduced into rice leaf protoplasts as described (Bart et al., 2006), while plasmids containing GAL4BD-VP16, pRTL, and 35sLUC were used as a positive control and plasmids containing GAL4BD, pRTL, and 35sLUC as a negative control. After incubation in the dark overnight, the luciferase activities were measured by the Dual-Luciferase Reporter Assay System (Promega) according to the manufacturer's instructions.

Transcriptional Activity Assay in Yeast

The open reading frame of *IPA1* and its C-terminal region (546 to 1254 bp) were amplified by the primer sets listed in Supplemental Table 2 online, cloned into *Xma*I and *Spe*I sites, and individually fused in frame to the GAL4 DNA binding domain in the vector pDBLeu (Gibco BRL). The fused constructs were transformed into Mav203 cells by the lithium acetate–mediated method. The transformed yeast (*Saccharomyces cerevisiae*) strains were plated on SD/–Leu medium at 28°C for 2 d. For the colony-lift filter assay (β-Galactosidase assay), the yeast cells were transferred to Whatman filter paper plus 5-bromo-4-chloro-3-indolyl-β-D-galactoside for transcription activation activity analysis within 8 h according to the manufacturer's instructions (Gibco BRL).

Yeast Two-Hybrid Assay

The coding sequence of *IPA1* was amplified by primer sets listed in Supplemental Table 2 online and cloned into pDEST-32 (Invitrogen), and *PCF1*, *PCF2*, Os *TB1*, and *TCP3* were cloned into pDEST-22 (Invitrogen). The fused constructs were transformed into Mav203 cells by the lithium acetate–mediated method. The transformed yeast strains were plated on SD/–Leu-Trp medium at 28°C for 2 d. For the colony-lift filter assay (β-Galactosidase assay), yeast cells were transferred to Whatman filter paper plus 5-bromo-4-chloro-3-indolyl-β-D-galactoside for transcription activation activity analysis within 8 h according to the manufacturer's instructions (Gibco BRL).

BiFC Assay

The coding sequence of *IPA1* was amplified by primer sets listed in Supplemental Table 2 online and cloned into puc-SCYCE (Bart et al., 2006), and *PCF1* and *PCF2* were cloned into puc-SCYNE(R) (Bart et al., 2006). The plasmid mixtures were introduced into rice leaf protoplasts as described (Bart et al., 2006). After incubation in the dark overnight, the fluorescence was observed with Olympus FluoView FV1000.

Expression and Purification of Fusion Proteins

The full-length *IPA1* cDNAs were amplified by the primer sets listed in Supplemental Table 2 online and cloned into the *Escherichia coli* expression vector pGEX 6p-1 (GE Healthcare) and pET28a. *PCF1*, *PCF2*, and Os *TB1* were cloned into pET-60-DEST (Merck). Expression of fusion proteins in BL21 transetta cells (Transgene) was induced with 0.3 mM isopropyl-1-thio-D-galactopyranoside at 12°C for 18 h. Fusion proteins were purified using Glutathione Sepharose 4 fast flow (GE Healthcare) or Ni Sepharose 6FF (GE Healthcare) and quantified by the Bio-Rad protein assay reagent and SDS-PAGE (see Supplemental Figure 25 online).

Labeling of DNA Fragments

Single-strand DNA probes were synthesized (see Supplemental Table 3 online) and purified by gel electrophoresis. Probes (100 ng of each fraction) were 3′ end-labeled with 10 μCi of [α-^{33}P]Deoxycytidine triphosphate using 1 unit of Klenow polymerase (Promega) at 37°C for 20 min in 10-μL reaction mixtures containing 50 mM Tris-HCl, pH 8.0, 5 mM $MgCl_2$, and 10 mM DTT. The ^{33}P-labeled probes were precipitated with 4 μL 3 M NaAC and 2 volumes of precold ethanol and dissolved into 15 μL of MilliQ water.

EMSA

^{33}P-labeled probes (1 μL of each) were incubated with purified proteins (1 μg fusion protein per reaction) in 20-μL mixtures containing 3 mM HEPES-potassium hydroxide, pH 7.9, 60 mM KCl, 0.15 mM EDTA, 1.5 mM DTT, 1.5% (v/v) glycerol, and 200 ng/mL poly(dI-dC) at room temperature for 20 min. After adding 5 μL of loading buffer (40 mM HEPES, pH 7.6, 200 mM KCl, 10 mM $MgCl_2$, 0.4 mM EDTA, 1 mM DTT, 20% [v/v] glycerol, and 0.25% [v/w] bromophenol blue), samples were subjected to electrophoresis on 4% SDS-PAGE gels running with 0.5× Tris-Borate-EDTA buffer at room temperature for 1 h. Labeled fragments and their shifted complexes with proteins were visualized in dried gels by phosphor imaging.

Real-Time PCR

Total RNAs were isolated from rice seedlings or YPs using a TRIzol kit (Invitrogen) according to the user manual. The RNA sample (1.6 μg) was treated with DNaseI and then used for cDNA synthesis with the SuperScript III first-strand cDNA synthesis system (Invitrogen) according to the manufacturer's instructions. Real-time PCR was performed using primer pairs (see Supplemental Table 4 online) in the EVER Green PCR Master Mix (Bio-Rad) with the Bio-Rad CFX96 real-time PCR detection system. PCR reactions were performed in triplicate for each sample, and expression levels were normalized to *Ubiquitin* or *Actin* for expression detection.

Accession Numbers

Sequence data from this article can be found in the GenBank/EMBL databases under the following accession numbers: IPA1, Os08g0509600; PCF1, Os04g0194600; PCF2, Os08g0544800; Os TB1, Os03g0706500; TCP3, Os01g0924400; DEP1, Os09g0441900; SLR1, Os03g0707600; LOG, Os01g0588900; PIN1b, Os02g0743400; FTL1, Os01g0218500; MADS56, Os10g0536100; Ubiquitin, Os03g0234200; and Actin, Os03g0718100.

Supplemental Data

The following materials are available in the online version of this article.

Supplemental Figure 1. Overview of ChIP Assays and ChIP-Seq Data.

Supplemental Figure 2. Overview of ChIP-Seq Results.

Supplemental Figure 3. Verification of ChIP-Seq Data.

Supplemental Figure 4. Heights of Overlapping and Nonoverlapping Peaks.

Supplemental Figure 5. Distribution of Peaks around Transcription Start Sites and Transcription End Sites.

Supplemental Figure 6. Binding Motifs Identified in IPA1 Binding Peaks in Four ChIP-Seq Assays.

Supplemental Figure 7. Density Plots of Different IPA1 Binding Motifs around Peak Summits in four ChIP-Seq Assays.

Supplemental Figure 8. Log Likelihood Ratio for Motif Peak Identification.

Supplemental Figure 9. Heights and LLR of GTAC and TGGGCC/T Motifs.

Supplemental Figure 10. LLR of Different Motifs in Overlapping and Nonoverlapping Peaks.

Supplemental Figure 11. Two Binding Motifs Showing Opposite Distribution Trends in IPA1 Binding Peaks in ChIP-SA rep 2 and ChIP-YP rep 2.

Supplemental Figure 12. Distribution of Peaks Divided by LLR of GTAC or TGGGCC/T in ChIP-SA rep 2 and ChIP-YP rep 2.

Supplemental Figure 13. Distribution of Peaks with Different Kinds of Motifs around the Transcription Start Site.

Supplemental Figure 14. Binding of His-IPA1 to TGGGCC/T Probe through Interacting with GST-PCF1 or GST-PCF2 in the EMSA Assay.

Supplemental Figure 15. Late-Flowering Phenotype of *IPA1*-Overexpressing Transgenic Plants.

Supplemental Figure 16. IPA1 Binding Profiles in Promoter Regions of *MADS56* and *FTL1*.

Supplemental Figure 17. Gene Numbers and Pathways of Genes Associated with IPA1 Binding Sites.

Supplemental Figure 18. Direct Binding of IPA1 to Promoters of *SLR1*, *LOG*, and *PIN1b*.

Supplemental Figure 19. IPA1 Binding Profile in Promoter of Os *TB1* in Four ChIP-Seq Results.

Supplemental Figure 20. Direct Binding of IPA1 to GTAC Core Sequence around the Subsummit in Os *TB1* Promoter.

Supplemental Figure 21. Os TB1 could Directly Bind Probes with TGGGCC/T Motif.

Supplemental Figure 22. IPA1 Binding Profile in Promoter of *DEP1* in Four ChIP-Seq Results.

Supplemental Figure 23. Direct Binding of IPA1 to GTAC Core Sequences around Subsummits in *DEP1* Promoter.

Supplemental Figure 24. Tiller and Branch Numbers per Main Panicle of Different RIL Lines.

Supplemental Figure 25. Purification of Fusion Proteins.

Supplemental Table 1. Primers for ChIP-qPCR.

Supplemental Table 2. Primers for Construction.

Supplemental Table 3. Primers for Generating Probes for EMSA.

Supplemental Table 4. Primers for Detecting the RNA level of Selected Genes.

Supplemental Methods 1. Motif Classification and Analysis of Peak Enrichment.

Supplemental Data Set 1A. Genes Associated with IPA1 Binding Sites Identified by ChIP-Seq in Shoot Apices.

Supplemental Data Set 1B. Genes Associated with IPA1 Binding Sites Identified by ChIP-Seq in Young Panicles.

Supplemental Data Set 1C. RNA-Seq Result with NIL-*IPA1* and NIP-*ipa1* in Shoot Apices.

Supplemental Data Set 1D. RNA-Seq Result with NIL-*IPA1* and NIP-*ipa1* in Young Panicles.

ACKNOWLEDGMENTS

We thank Shouyi Chen (Institute of Genetics and Developmental Biology, Chinese Academy of Science) for providing the plasmids GAL4BD, 35sLUC, and pRTL and Zhengjin Xu (Rice Research Institute, Shenyang Agricultural University) for the rice variety *LJ5*. We thank the Genomics and Bioinformatics Facility of State Key Laboratory of Plant Genomics, Institute of Genetic and Developmental Biology for sequencing. This work was supported by grants from the Ministry of Science and Technology of China (2013CBA01401) and the Ministry of Agriculture of China (2011ZX08001-004).

AUTHOR CONTRIBUTIONS

Z.L., G.X., and J.L. conceived this project and designed all experiments. Z.L., H.Y., J.W., Y.Q.J., G.L., X.H., Q.Q., and Y.H.J. performed experiments. Z.L., H.Y., Y.W., G.X., X.F., and J.L. analyzed data. Z.L., H.Y., and J.L. wrote the article.

Received May 14, 2013; revised September 27, 2013; accepted October 7, 2013; published October 29, 2013.

REFERENCES

Arite, T., Iwata, H., Ohshima, K., Maekawa, M., Nakajima, M., Kojima, M., Sakakibara, H., and Kyozuka, J. (2007). *DWARF10*, an *RMS1/MAX4/DAD1* ortholog, controls lateral bud outgrowth in rice. Plant J. **51:** 1019–1029.

Arite, T., Umehara, M., Ishikawa, S., Hanada, A., Maekawa, M., Yamaguchi, S., and Kyozuka, J. (2009). *d14*, a strigolactone-insensitive mutant of rice, shows an accelerated outgrowth of tillers. Plant Cell Physiol. **50:** 1416–1424.

Ashburner, M., et al; The Gene Ontology Consortium (2000). Gene ontology: Tool for the unification of biology. Nat. Genet. **25:** 25–29.

Ashikari, M., Sakakibara, H., Lin, S., Yamamoto, T., Takashi, T., Nishimura, A., Angeles, E.R., Qian, Q., Kitano, H., and Matsuoka, M. (2005). Cytokinin oxidase regulates rice grain production. Science **309:** 741–745.

Avraham, S., et al. (2008). The Plant Ontology Database: A community resource for plant structure and developmental stages controlled vocabulary and annotations. Nucleic Acids Res. **36** (Database issue)**:** D449–D454.

Bailey, T.L. (2011). DREME: Motif discovery in transcription factor ChIP-seq data. Bioinformatics **27:** 1653–1659.

Bart, R., Chern, M., Park, C.J., Bartley, L., and Ronald, P.C. (2006). A novel system for gene silencing using siRNAs in rice leaf and stem-derived protoplasts. Plant Methods **2:** 13.

Birkenbihl, R.P., Jach, G., Saedler, H., and Huijser, P. (2005). Functional dissection of the plant-specific SBP-domain: Overlap of the DNA-binding and nuclear localization domains. J. Mol. Biol. **352:** 585–596.

Bolduc, N., Yilmaz, A., Mejia-Guerra, M.K., Morohashi, K., O'Connor, D., Grotewold, E., and Hake, S. (2012). Unraveling the KNOTTED1 regulatory network in maize meristems. Genes Dev. **26:** 1685–1690.

Busch, W., et al. (2010). Transcriptional control of a plant stem cell niche. Dev. Cell **18:** 849–861.

Donald, C. (1968). The breeding of crop ideotypes. Euphytica **17:** 385–403.

Dun, E.A., de Saint Germain, A., Rameau, C., and Beveridge, C.A. (2012). Antagonistic action of strigolactone and cytokinin in bud outgrowth control. Plant Physiol. **158:** 487–498.

Fornara, F., and Coupland, G. (2009). Plant phase transitions make a SPLash. Cell **138:** 625–627.

Gandikota, M., Birkenbihl, R.P., Höhmann, S., Cardon, G.H., Saedler, H., and Huijser, P. (2007). The miRNA156/157 recognition element in the 3′ UTR of the *Arabidopsis* SBP box gene *SPL3* prevents early flowering by translational inhibition in seedlings. Plant J. **49:** 683–693.

Gou, J.Y., Felippes, F.F., Liu, C.J., Weigel, D., and Wang, J.W. (2011). Negative regulation of anthocyanin biosynthesis in *Arabidopsis* by a miR156-targeted SPL transcription factor. Plant Cell **23:** 1512–1522.

Guo, J., Song, J., Wang, F., and Zhang, X.S. (2007). Genome-wide identification and expression analysis of rice cell cycle genes. Plant Mol. Biol. **64:** 349–360.

Guo, S., Xu, Y., Liu, H., Mao, Z., Zhang, C., Ma, Y., Zhang, Q., Meng, Z., and Chong, K. (2013). The interaction between OsMADS57 and OsTB1 modulates rice tillering via *DWARF14*. Nat. Commun. **4:** 1566.

Hu, M., Yu, J., Taylor, J.M., Chinnaiyan, A.M., and Qin, Z.S. (2010). On the detection and refinement of transcription factor binding sites using ChIP-Seq data. Nucleic Acids Res. **38:** 2154–2167.

Huang, X., Qian, Q., Liu, Z., Sun, H., He, S., Luo, D., Xia, G., Chu, C., Li, J., and Fu, X. (2009). Natural variation at the *DEP1* locus enhances grain yield in rice. Nat. Genet. **41:** 494–497.

Ikeda, A., Ueguchi-Tanaka, M., Sonoda, Y., Kitano, H., Koshioka, M., Futsuhara, Y., Matsuoka, M., and Yamaguchi, J. (2001). *slender rice*, a constitutive gibberellin response mutant, is caused by a null mutation of the *SLR1* gene, an ortholog of the height-regulating gene *GAI*/*RGA*/*RHT*/*D8*. Plant Cell **13:** 999–1010.

Ishikawa, S., Maekawa, M., Arite, T., Onishi, K., Takamure, I., and Kyozuka, J. (2005). Suppression of tiller bud activity in tillering dwarf mutants of rice. Plant Cell Physiol. **46:** 79–86.

Jaiswal, P., Ware, D., Ni, J., Chang, K., Zhao, W., Schmidt, S., Pan, X., Clark, K., Teytelman, L., Cartinhour, S., Stein, L., and McCouch, S. (2002). Gramene: Development and integration of trait and gene ontologies for rice. Comp. Funct. Genomics **3:** 132–136.

Jansen, R., Yu, H., Greenbaum, D., Kluger, Y., Krogan, N.J., Chung, S., Emili, A., Snyder, M., Greenblatt, J.F., and Gerstein, M. (2003). A Bayesian networks approach for predicting protein-protein interactions from genomic data. Science **302:** 449–453.

Jeong, D.H., Park, S., Zhai, J., Gurazada, S.G., De Paoli, E., Meyers, B.C., and Green, P.J. (2011). Massive analysis of rice small RNAs: Mechanistic implications of regulated microRNAs and variants for differential target RNA cleavage. Plant Cell **23:** 4185–4207.

Jiao, Y., Wang, Y., Xue, D., Wang, J., Yan, M., Liu, G., Dong, G., Zeng, D., Lu, Z., Zhu, X., Qian, Q., and Li, J. (2010). Regulation of *OsSPL14* by OsmiR156 defines ideal plant architecture in rice. Nat. Genet. **42:** 541–544.

Johnson, D.S., et al. (2008). Systematic evaluation of variability in ChIP-chip experiments using predefined DNA targets. Genome Res. **18:** 393–403.

Kanehisa, M., Goto, S., Sato, Y., Furumichi, M., and Tanabe, M. (2012). KEGG for integration and interpretation of large-scale molecular data sets. Nucleic Acids Res. **40** (Database issue)**:** D109–D114.

Khush, G.S. (1995). Breaking the yield frontier of rice. GeoJournal **35:** 329–332.

Kobayashi, K., Yasuno, N., Sato, Y., Yoda, M., Yamazaki, R., Kimizu, M., Yoshida, H., Nagamura, Y., and Kyozuka, J. (2012). Inflorescence meristem identity in rice is specified by overlapping functions of three *AP1*/*FUL*-like MADS box genes and *PAP2*, a *SEPALLATA* MADS box gene. Plant Cell **24:** 1848–1859.

Kosugi, S., and Ohashi, Y. (1997). PCF1 and PCF2 specifically bind to *cis* elements in the rice proliferating cell nuclear antigen gene. Plant Cell **9:** 1607–1619.

Kurakawa, T., Ueda, N., Maekawa, M., Kobayashi, K., Kojima, M., Nagato, Y., Sakakibara, H., and Kyozuka, J. (2007). Direct control of shoot meristem activity by a cytokinin-activating enzyme. Nature **445:** 652–655.

Landt, S.G., et al. (2012). ChIP-seq guidelines and practices of the ENCODE and modENCODE consortia. Genome Res. **22:** 1813–1831.

Lee, J., He, K., Stolc, V., Lee, H., Figueroa, P., Gao, Y., Tongprasit, W., Zhao, H., Lee, I., and Deng, X.W. (2007). Analysis of transcription factor HY5 genomic binding sites revealed its hierarchical role in light regulation of development. Plant Cell **19:** 731–749.

Li, G., Hall, T.C., and Holmes-Davis, R. (2002). Plant chromatin: Development and gene control. Bioessays **24:** 234–243.

Li, R., Yu, C., Li, Y., Lam, T.W., Yiu, S.M., Kristiansen, K., and Wang, J. (2009). SOAP2: An improved ultrafast tool for short read alignment. Bioinformatics **25:** 1966–1967.

Lin, H., Wang, R., Qian, Q., Yan, M., Meng, X., Fu, Z., Yan, C., Jiang, B., Su, Z., Li, J., and Wang, Y. (2009). DWARF27, an iron-containing protein required for the biosynthesis of strigolactones, regulates rice tiller bud outgrowth. Plant Cell **21:** 1512–1525.

Martín-Trillo, M., and Cubas, P. (2010). TCP genes: A family snapshot ten years later. Trends Plant Sci. **15:** 31–39.

Minakuchi, K., Kameoka, H., Yasuno, N., Umehara, M., Luo, L., Kobayashi, K., Hanada, A., Ueno, K., Asami, T., Yamaguchi, S., and Kyozuka, J. (2010). *FINE CULM1* (*FC1*) works downstream of strigolactones to inhibit the outgrowth of axillary buds in rice. Plant Cell Physiol. **51:** 1127–1135.

Miura, K., Ikeda, M., Matsubara, A., Song, X.J., Ito, M., Asano, K., Matsuoka, M., Kitano, H., and Ashikari, M. (2010). *OsSPL14* promotes panicle branching and higher grain productivity in rice. Nat. Genet. **42:** 545–549.

Niwa, M., Daimon, Y., Kurotani, K., Higo, A., Pruneda-Paz, J.L., Breton, G., Mitsuda, N., Kay, S.A., Ohme-Takagi, M., Endo, M., and Araki, T. (2013). BRANCHED1 interacts with FLOWERING LOCUS T to repress the floral transition of the axillary meristems in *Arabidopsis*. Plant Cell **25:** 1228–1242.

Oh, E., Yamaguchi, S., Hu, J., Yusuke, J., Jung, B., Paik, I., Lee, H.S., Sun, T.P., Kamiya, Y., and Choi, G. (2007). PIL5, a phytochrome-interacting bHLH protein, regulates gibberellin responsiveness by binding directly to the *GAI* and *RGA* promoters in *Arabidopsis* seeds. Plant Cell **19:** 1192–1208.

Ouyang, S., et al. (2007). The TIGR Rice Genome Annotation Resource: Improvements and new features. Nucleic Acids Res. **35** (Database issue)**:** D883–D887.

Pujar, A., et al. (2006). Whole-plant growth stage ontology for angiosperms and its application in plant biology. Plant Physiol. **142:** 414–428.

Qiao, Y., Piao, R., Shi, J., Lee, S.I., Jiang, W., Kim, B.K., Lee, J., Han, L., Ma, W., and Koh, H.J. (2011). Fine mapping and candidate gene analysis of *dense and erect panicle 3, DEP3*, which confers high grain yield in rice (*Oryza sativa* L.). Theor. Appl. Genet. **122:** 1439–1449.

Rao, N.N., Prasad, K., Kumar, P.R., and Vijayraghavan, U. (2008). Distinct regulatory role for *RFL*, the rice *LFY* homolog, in determining flowering time and plant architecture. Proc. Natl. Acad. Sci. USA **105:** 3646–3651.

Reyes, J.C., Hennig, L., and Gruissem, W. (2002). Chromatin-remodeling and memory factors. New regulators of plant development. Plant Physiol. **130:** 1090–1101.

Rhodes, D.R., Tomlins, S.A., Varambally, S., Mahavisno, V., Barrette, T., Kalyana-Sundaram, S., Ghosh, D., Pandey, A., and Chinnaiyan, A.M. (2005). Probabilistic model of the human protein-protein interaction network. Nat. Biotechnol. **23:** 951–959.

Saleh, A., Alvarez-Venegas, R., and Avramova, Z. (2008). An efficient chromatin immunoprecipitation (ChIP) protocol for studying histone modifications in *Arabidopsis* plants. Nat. Protoc. **3:** 1018–1025.

Sasaki, A., Ashikari, M., Ueguchi-Tanaka, M., Itoh, H., Nishimura, A., Swapan, D., Ishiyama, K., Saito, T., Kobayashi, M., Khush, G.S., Kitano, H., and Matsuoka, M. (2002). Green revolution: A mutant gibberellin-synthesis gene in rice. Nature **416:** 701–702.

Sasaki, A., Itoh, H., Gomi, K., Ueguchi-Tanaka, M., Ishiyama, K., Kobayashi, M., Jeong, D.H., An, G., Kitano, H., Ashikari, M., and Matsuoka, M. (2003). Accumulation of phosphorylated repressor for gibberellin signaling in an F-box mutant. Science **299:** 1896–1898.

Spitz, F., and Furlong, E.E. (2012). Transcription factors: From enhancer binding to developmental control. Nat. Rev. Genet. **13:** 613–626.

Sun, Y., et al. (2010). Integration of brassinosteroid signal transduction with the transcription network for plant growth regulation in *Arabidopsis*. Dev. Cell **19:** 765–777.

Takeda, T., Suwa, Y., Suzuki, M., Kitano, H., Ueguchi-Tanaka, M., Ashikari, M., Matsuoka, M., and Ueguchi, C. (2003). The *OsTB1* gene negatively regulates lateral branching in rice. Plant J. **33:** 513–520.

Trapnell, C., Pachter, L., and Salzberg, S.L. (2009). TopHat: Discovering splice junctions with RNA-Seq. Bioinformatics **25:** 1105–1111.

Trapnell, C., Roberts, A., Goff, L., Pertea, G., Kim, D., Kelley, D.R., Pimentel, H., Salzberg, S.L., Rinn, J.L., and Pachter, L. (2012). Differential gene and transcript expression analysis of RNA-seq experiments with TopHat and Cufflinks. Nat. Protoc. **7:** 562–578.

Trapnell, C., Williams, B.A., Pertea, G., Mortazavi, A., Kwan, G., van Baren, M.J., Salzberg, S.L., Wold, B.J., and Pachter, L. (2010). Transcript assembly and quantification by RNA-Seq reveals unannotated transcripts and isoform switching during cell differentiation. Nat. Biotechnol. **28:** 511–515.

Ueguchi-Tanaka, M., Ashikari, M., Nakajima, M., Itoh, H., Katoh, E., Kobayashi, M., Chow, T.Y., Hsing, Y.I., Kitano, H., Yamaguchi, I., and Matsuoka, M. (2005). *GIBBERELLIN INSENSITIVE DWARF1* encodes a soluble receptor for gibberellin. Nature **437:** 693–698.

Unte, U.S., Sorensen, A.M., Pesaresi, P., Gandikota, M., Leister, D., Saedler, H., and Huijser, P. (2003). *SPL8*, an SBP-box gene that affects pollen sac development in *Arabidopsis*. Plant Cell **15:** 1009–1019.

Valouev, A., Johnson, D.S., Sundquist, A., Medina, C., Anton, E., Batzoglou, S., Myers, R.M., and Sidow, A. (2008). Genome-wide analysis of transcription factor binding sites based on ChIP-Seq data. Nat. Methods **5:** 829–834.

Virk, P., Khush, G., and Peng, S. (2004). Breeding to enhance yield potential of rice at IRRI: The ideotype approach. Int. Rice Res. Notes **29:** 5–9.

Wang, J.W., Czech, B., and Weigel, D. (2009). MiR156-regulated SPL transcription factors define an endogenous flowering pathway in *Arabidopsis thaliana*. Cell **138:** 738–749.

Wang, S., Wu, K., Yuan, Q., Liu, X., Liu, Z., Lin, X., Zeng, R., Zhu, H., Dong, G., Qian, Q., Zhang, G., and Fu, X. (2012). Control of grain size, shape and quality by *OsSPL16* in rice. Nat. Genet. **44:** 950–954.

Wang, Y., and Li, J. (2008). Molecular basis of plant architecture. Annu. Rev. Plant Biol. **59:** 253–279.

Winter, C.M., et al. (2011). LEAFY target genes reveal floral regulatory logic, cis motifs, and a link to biotic stimulus response. Dev. Cell **20:** 430–443.

Wu, G., Park, M.Y., Conway, S.R., Wang, J.W., Weigel, D., and Poethig, R.S. (2009). The sequential action of miR156 and miR172 regulates developmental timing in *Arabidopsis*. Cell **138:** 750–759.

Wu, G., and Poethig, R.S. (2006). Temporal regulation of shoot development in *Arabidopsis thaliana* by miR156 and its target *SPL3*. Development **133:** 3539–3547.

Yamaguchi, A., Wu, M.F., Yang, L., Wu, G., Poethig, R.S., and Wagner, D. (2009). The microRNA-regulated SBP-Box transcription factor SPL3 is a direct upstream activator of *LEAFY, FRUITFULL*, and *APETALA1*. Dev. Cell **17:** 268–278.

Yamasaki, K., et al. (2004). A novel zinc-binding motif revealed by solution structures of DNA-binding domains of *Arabidopsis* SBP-family transcription factors. J. Mol. Biol. **337:** 49–63.

Youens-Clark, K., et al. (2011). Gramene database in 2010: Updates and extensions. Nucleic Acids Res. **39** (Database issue)**:** D1085–D1094.

Yu, H., Huang, J., Qiao, N., Green, C.D., and Han, J.D. (2010). Evaluating diabetes and hypertension disease causality using mouse phenotypes. BMC Syst. Biol. **4:** 97.

Yu, N., Cai, W.J., Wang, S., Shan, C.M., Wang, L.J., and Chen, X.Y. (2010). Temporal control of trichome distribution by microRNA156-targeted *SPL* genes in *Arabidopsis thaliana*. Plant Cell **22:** 2322–2335.

Zhang, Y., Liu, T., Meyer, C.A., Eeckhoute, J., Johnson, D.S., Bernstein, B.E., Nusbaum, C., Myers, R.M., Brown, M., Li, W., and Liu, X.S. (2008). Model-based analysis of ChIP-Seq (MACS). Genome Biol. **9:** R137.

Zhang, Y., Mayba, O., Pfeiffer, A., Shi, H., Tepperman, J.M., Speed, T.P., and Quail, P.H. (2013). A quartet of PIF bHLH factors provides a transcriptionally centered signaling hub that regulates seedling morphogenesis through differential expression-patterning of shared target genes in *Arabidopsis*. PLoS Genet. **9:** e1003244.

Zheng, Y., Ren, N., Wang, H., Stromberg, A.J., and Perry, S.E. (2009). Global identification of targets of the *Arabidopsis* MADS domain protein AGAMOUS-Like15. Plant Cell **21:** 2563–2577.

Zhu, Y., et al. (2006). *ELONGATED UPPERMOST INTERNODE* encodes a cytochrome P450 monooxygenase that epoxidizes gibberellins in a novel deactivation reaction in rice. Plant Cell **18:** 442–456.

Zou, J., Chen, Z., Zhang, S., Zhang, W., Jiang, G., Zhao, X., Zhai, W., Pan, X., and Zhu, L. (2005). Characterizations and fine mapping of a mutant gene for high tillering and dwarf in rice (*Oryza sativa* L.). Planta **222:** 604–612.